# Reliability analysis of riverbank stability accounting for the intrinsic variability of unsaturated soil parameters


Reliability analysis of riverbank stability accounting for the intrinsic variability of unsaturated soil parameters / Guido Gottardi, Carmine G. Gragnano, Marco Ranalli, Laura Tonni. - In: STRUCTURAL SAFETY. - ISSN 0167-4730. - ELETTRONICO. - 86:September 2020(2020), pp. 101973.1-101973.13. [10.1016/j.strusafe.2020.101973]


DOI: http://doi.org/10.1016/j.strusafe.2020.101973

*Article Title:*

# Reliability analysis of riverbank stability accounting for the intrinsic variability of unsaturated soil parameters

*Journal Name:*

**Structural Safety**

*Authors:*

**Guido Gottardi[a,*], Carmine G. Gragnano[b], Marco Ranalli[c], Laura Tonni[d]**

[a,]*Corresponding Author, *Department of Civil, Chemical, Environmental and Materials Engineering, DICAM, Alma Mater Studiorum - University of Bologna.* Viale Risorgimento 2, 40136 Bologna (Italy). Phone: +39 0512093524.
E-mail: guido.gottardi2@unibo.it

[b]*Department of Civil, Chemical, Environmental and Materials Engineering, DICAM, Alma Mater Studiorum - University of Bologna.* Viale Risorgimento 2, 40136 Bologna (Italy).
E-mail: carmine.gragnano2@unibo.it

[c]*Department of Civil, Chemical, Environmental and Materials Engineering, DICAM, Alma Mater Studiorum - University of Bologna.* Viale Risorgimento 2, 40136 Bologna (Italy).
E-mail: marco.ranalli@unibo.it

[d]*Department of Civil, Chemical, Environmental and Materials Engineering, DICAM, Alma Mater Studiorum - University of Bologna.* Viale Risorgimento 2, 40136 Bologna (Italy).
E-mail: laura.tonni@unibo.it
ORCID 0000-0002-9391-6661

# Abstract

The paper presents a probabilistic study aimed at investigating the role of the soil hydraulic response on the stability of existing river embankments, for which the uncertainty and the inherent variability of geotechnical and hydraulic properties are typically greater when compared to new flood defence structures. The study has been carried out with reference to a specific, thoroughly investigated 20 m-long segment of the river Secchia banks (northern Italy), which experienced a catastrophic sudden failure after a period of intense rainfall, in January 2014. By taking such well-documented case as a base, the proposed probabilistic analyses consider three key aspects, typically disregarded in routine risk assessment procedures: i) transient seepage flow through earth structures due to time dependent hydraulic loads, ii) unsaturated conditions of soils forming the river embankment, iii) uncertainty of the soil model parameters, with special emphasis placed on the impact of intrinsic variability of unsaturated soil parameters. The numerical results, obtained from the application of the *Point Estimate Method*, allow identifying the crucial role of suction distribution on the probability of failure of the riverbank slopes and clearly show that such probability can be significantly underestimated when the variability of hydraulic parameters is neglected.



**Keywords:** unsaturated soil, transient seepage, probabilistic analysis, Point Estimate Method, riverbank stability

# 1. Introduction

The evaluation of riverbank stability represents a fundamental task in georisk assessment. Indeed, overestimating the safety margin of a flood defence structure may potentially lead to totally unexpected failures and subsequent severe consequences in terms of damages, repairing costs and human losses. Hence, a thorough understanding of the different factors adversely affecting riverbank stability and the way they interact to determine failure conditions is a necessary step for engineers in order to design successful and cost-effective countermeasures against potential collapses.

In recent years, the use of numerical methods has offered a powerful means to develop accurate groundwater seepage models, enabling transient analyses coupled with unsaturated stress approaches for the evaluation of the dynamic distribution of pore water pressure due to rainfall events, evaporation and river level fluctuations. A number of studies ([1-2] among others), based on different numerical approaches, have thus investigated in great detail the effect of changes in pore water pressures on the riverbank stability, with special attention paid to the crucial role of matric suction and its influence on the soil properties in the partially saturated zone of the embankment.

At the same time, numerical analysis has proved to be a suitable and effective tool in order to take into account a further fundamental geotechnical issue, that is the intrinsic variability of soils properties, even in relatively homogeneous deposits, together with the unavoidable uncertainties due to limited experimental data and to the related correlation models adopted for soil characterization [3-8].

A large number of research contributions (e.g. [9-14]), based on either theoretical applications or failure case studies, have discussed the effect of uncertainties and spatial variation of soil shear strength on slope analysis reliability, whilst only few available studies have also considered the variability of hydraulic properties, particularly those governing the behaviour of unsaturated soils [15-16]. An even more limited number of published works [17] have actually tackled the problem with reference to existing river embankments and a substantial lack of applications to relevant case studies is thus observed. However, in these structures the spatial variability of hydraulic properties, especially in unsaturated soil conditions, may remarkably affect both the seepage regime [18-19], which results in specific flow paths, and the unsaturated soil shear strength [20], with significant implications on the overall stability.

In order to gain a better insight into such geotechnical issues, this paper presents an extensive probabilistic study specifically aimed at investigating the role of the intrinsic variability of unsaturated soil hydraulic properties in the assessment of existing riverbank safety conditions. The study has been carried out using the geotechnical dataset collected along a 20 m bank segment of the Secchia river, a right tributary of the major Po river, north of the historic town of Modena (Italy). Following the catastrophic failure occurred in January 2014 [21], this river embankment segment was thoroughly investigated by means of in situ and laboratory tests and a valuable and varied database has thus become available for the analyses. Starting from such well-documented real case, the objective of the study is primarily to examine the effect of different geotechnical sources of uncertainties on riverbank stability, with specific emphasis on the crucial impact of intrinsic variability of unsaturated soil hydraulic parameters. After a brief summary of the *Point Estimate Method* (PEM), which is the probabilistic approach adopted in this numerical study, and of the accurate geotechnical characterization of the sediments forming the whole river embankment system, the paper first presents the results of a few preliminary limit equilibrium analyses under steady-state seepage conditions, assuming soil shear strength as the only source of uncertainty. Next, two further series of limit equilibrium analyses, performed under transient flow conditions as induced by fluctuating river levels and rainfall events, are shown and the effect of assuming hydraulic parameters either as deterministic or random variables is discussed with respect to the resulting probability of riverbank failure. As regards the specific collapse that led to the January 2014 large breach in the Secchia river embankment, it is worth observing that in such case the triggering mechanism was eventually ascribed to a potential local lack of structural integrity induced by animal burrows [21], which is outside the scope of this study and therefore it will not be considered in the following analyses. However, the localised damages observed in the surroundings of the failed section, coupled with the reduction in saturation degree and suction caused by persistent and ever increasing high water events, have shown the need to further explore the actual factors affecting the potential riverbank instability and to provide a rational methodological approach to take into account the unavoidable intrinsic variability of the soil parameters which control the local conditions.

## 2. Uncertainty propagation methods

The uncertainty propagation analysis allows propagating the errors from input data (e.g. mechanical properties, retention and hydraulic soil parameters) to the final result (i.e. the factor of safety and the probability of failure in ultimate limit state analyses). In geotechnical practice and research, a number of simplified uncertainty propagation methods, like *First Order Second Moment Method* (FOSM), *Point Estimate Method* (PEM) or *First Order Reliability Method* (FORM) have long been successfully adopted (e.g. [9,22-25]). Such approaches are often used as a valid alternative to more accurate and well-established procedures, typically the *Monte Carlo Method* (MCM), which turn out to be more difficult to be implemented and very time-consuming when adopted in slope stability analyses based on Limit Equilibrium or Finite Element methods [25]. In addition to the simplified FOSM, PEM and FORM mentioned above, in recent years advanced stochastic approaches, capable of combining accuracy with computational efficiency, have been also proposed in the literature with the aim of overcoming the prohibitive time and resources efforts required by the direct MCM. Among them, it is worth mentioning the *Stochastic Response Surface Method* [26] and, in particular, the *Subset Simulation* [27-29]. However, although these latest computational strategies have been devised to alleviate and facilitate the application of probability-based approaches in slope assessment, their use in routine engineering practice is still far from being widespread, probably due to complexity of the relevant implementation algorithms. Some authors (e.g. [28]) also observed that *Subset Simulation* still requires a significant computational cost at extremely small probability levels (e.g., probability of failure $P_f < 10^{-4} \sim 10^{-5}$).

At the same time the simplified methods, though approximated, appear to provide a valid, efficient and relatively easy tool to incorporate spatial variability of soil properties into reliability analysis and risk assessment of slope stability, especially when failure probability is not very low. In this case, indeed, such methods typically result in an approximate but not erroneous estimate of the probability of failure. Regarding this point, it is worth observing also that the accuracy of the computed probability of failure largely depends on the reliability of the statistical characterization of the input parameters, and that the estimates of the probability of failure should be interpreted in terms of their order of magnitude, as emphasized by Duncan and Sleep [30].

In this work, the *Point Estimate Method* in particular was used as probabilistic procedure to propagate the uncertainty from the geotechnical and hydraulic soil properties to the probability of failure ($P_f$) of the riverbank slopes. Computational efficiency, together with a rather straightforward implementation procedure, caused PEM to be selected instead of MCM. In spite of a certain "roughness" of the adopted method, a few preliminary analyses, carried out with both PEM and MCM and accounting for the only uncertainties on soil shear strength, led to numerically different results, lying however in the same order of magnitude. This outcome, obtained for values of $P_f$ relatively high, cannot be obviously considered as generally valid.

The *Point Estimate Method* is widely used when no closed-form analytical solutions are available and a number of successful applications of the method [31-33] to typical geotechnical stability problems, either using Limit Equilibrium Method (LEM) or the Finite Element Method (FEM), can be found in the literature. Furthermore, in recent years the PEM has been implemented in a number of commercial codes that are commonly used for stability analyses, hence its use is very likely to earn popularity among engineers also for routine applications.

## 2.1 Adopted probabilistic approach

The *Point Estimate Method* consists in replacing the continuous random variables, characterized by a probability density function, with discrete random variables described by two or more points with assigned weight. The discrete points and the relevant weights are estimated on the basis of the statistical moments of the continuous random variables, i.e. mean value, variance and skewness coefficient.

The original PEM [34-36] allowed considering such first three statistical moments only in case of function of a single random variable; in case of multiple variables, the application of the method was restricted to systems of correlated and symmetrically distributed random variables. The later formulation developed by Panchalingam and Harr [37] allowed incorporating both correlated and skewed random variables into the uncertainty analysis in the case of multivariate random variables problems as well. The key features of the method are briefly summarized below.

Let $f(X) = f(X_1, X_2, \ldots, X_N)$ be a function of $N$ correlated and skewed random variables. The first three statistical moments (mean, standard deviation and skewness coefficient) and the correlation structure of random variables are assumed to be known.

The method firstly defines the point estimate locations through the statistical moments of the random variables. For each random variable, two point estimate locations are evaluated, according to the following relationships:

$$X_+ = \mu_X + \left[\frac{\nu_X}{2} + \sqrt{1 + \left(\frac{\nu_X}{2}\right)^2}\right]\sigma_X \tag{1}$$

$$X_- = \mu_X + \left[\frac{\nu_X}{2} - \sqrt{1 + \left(\frac{\nu_X}{2}\right)^2}\right]\sigma_X \tag{2}$$

where $\mu_X$ is the mean value, $\sigma_X$ is the standard deviation and $\nu_X$ is the skewness coefficient.

Estimate locations $X_+$ and $X_-$ are then associated with weights $P_+$ and $P_-$ respectively. These are given by:

$$P_+ = \frac{1}{2}\left[1 - \frac{\nu_X}{2}\frac{1}{\sqrt{1+(\nu_X/2)^2}}\right] \tag{3}$$

$$P_- = 1 - P_+ \tag{4}$$

For a function of $N$ random variables, the method provides $2^N$ point estimate locations, resulting from all possible combinations of point estimate locations. Accordingly, the weight associated with a general combination ($X_{1\pm}$, $X_{2\pm}$, …, $X_{N\pm}$) is defined as:

(5) $$P_{\pm\pm\cdots\pm} = P_{1\pm}P_{2\pm} \dots P_{N\pm} + \sum_{i=1}^{N-1}\sum_{j=i+1}^{N}(\pm)_i(\pm)_j a_{ij}P_{ij}$$

where $a_{ij} = \rho_{ij}\ (P_{i+}P_{i-}P_{j+}P_{j-})^{0.5}$, $\rho_{ij}$ = correlation coefficient between the random variables $X_i$ and $X_j$, $P_{ij} = P_{1\pm}P_{2\pm}\dots P_{k\pm}\dots P_{N\pm}$ ($k \neq i$ and $k \neq j$).

The statistical m-th moment of the function $f(X)$ can be therefore expressed as follows:

(6) $$E[f(x)^m] \approx \sum_{j=1}^{k} P_j f\left(X_j\right)^m$$

where $k$ is the number of point estimate locations, $P_j$ is the weight associated with combination $j$, $f(X_j)$ is the function evaluated at point estimate location $j$. In particular, the mean $\mu_{f(X)}$ and the variance $\sigma^2_{f(X)}$ of the function can be then estimated according to the following relationships:

(7) $$\mu_{f(X)} = E[f(x)]$$

(8) $$\sigma^2_{f(X)} = E[f(X)^2] - (E[f(x)])^2$$

Finally, the reliability index $\beta$ and the probability of failure $P_f$ are given by:

(9) $$\beta = \frac{\mu_{SF}-1}{\sigma_{SF}}$$

(10) $$P_f = 1 - \Phi(\beta)$$

where $\Phi$ is the cumulative distribution of the standard normal random variable. A Normal probability distribution of the safety factor is assumed in order to obtain the probability of failure.

# 3. Reference case study

The probabilistic study proposed in this paper was carried out with reference to a specific, thoroughly investigated 20 m-long segment of the river Secchia banks (northern Italy), which suddenly collapsed after a period of intense rainfall, in January 2014 (Figure 1). This section provides a brief description of the detailed and rather varied geotechnical database collected after the bank failure in order to obtain information related to the collapse and used as reference dataset for the analyses contained herein.

As shown in Figure 2, the site investigation campaign was carried out along three main representative alignments: the first alignment was selected upstream from the collapsed river embankment section, approximately 900 m distant from the breach, the second was located in front of the collapsed area, on the opposite river embankment, whilst the third was placed next to the breach, only a few meters away on the downriver side. For each alignment, a borehole (BH) and a seismic piezocone test (SCPTU) were carried out from the crest of the river embankment and pushed to approximately 30 m in depth; two additional piezocone tests (CPTU) were carried out at the berm and close to the outer slope toe. The latter tests were stopped at different depths, from 14 to 26 m, depending on their position on the river embankment. A few dissipation tests were also carried out along each piezocone vertical, in order to monitor the pore water pressure decay with time and to evaluate the consolidation characteristics of fine sediments.

The laboratory experimental programme, carried out on a total of 27 undisturbed soil samples, included a significant number of tests for the determination of basic physical properties of soils, Atterberg limits, particle size distribution, in conjunction with a few oedometer tests, direct shear tests, drained (TXCD) and undrained (TXCU) triaxial tests to estimate the mechanical parameters of sediments. In addition, series of evaporation tests were performed for the estimation of the retention and hydraulic properties of the river embankment soil in partially-saturated conditions.

## 3.1 In situ testing interpretation

The subsoil beneath the collapsed river embankment stretch mainly consists of Pleistocene alluvial sediments resulting from depositional and erosional process of the Secchia and Panaro rivers, both draining a significant part of the Emilian Apennines into the major Italian watercourse Po.

Figure 3 shows the profiles of the corrected cone resistance $q_t$, sleeve friction $f_s$ and pore pressure $u$

obtained from the representative piezocone test SCPTU 7, located on the river embankment crest in Section No. 3, the latter being depicted here according to its geometry after collapse. The interpretation of piezocone data in terms of the well-known classification framework proposed by Robertson [38], aimed at identifying the in situ Soil Behaviour Type (*SBT)*, and the actual soil stratigraphy provided by the adjacent borehole BH-3 are also reported in the figure. Despite a few discrepancies observed between CPTU-based classification results and the stratigraphy from boreholes, presumably due to the combined effect of suction above phreatic surface, simplified evaluation of effective stress state within the bank and partial drainage during cone penetration testing [39], the comparative analysis of field data allows identifying three main soil units. As shown in Figure 4 with respect to the cross-section No. 3, the stratigraphic arrangement includes:

- a 5 m thick, rather heterogeneous top layer of sands, silty sands and sandy silts (labelled as *Unit R*), forming the artificial river embankment;
- a predominantly silty unit (*Unit B*), 5 to 12 m thick, referable to the flood plain environment and corresponding to the upper part of the river embankment foundation subsoil;
- a clayey layer, detected at 12 to 30 m in depth from the bank crest, labelled as *Unit C*.

In this stratigraphic scheme, the groundwater table is located at approximately 6 m from the crest of the reshaped bank, at 30 m above mean sea level, i.e. close to the transition surface between *Unit R* and *Unit B,* as suggested by field data provided by the Casagrande-type piezometer installed into borehole BH-3 as well as by interpretation of CPTU pore pressure profiles. Such phreatic surface was found to be slightly sloping landwards, the hydraulic gradient *i* being equal to 4%. Similar stratigraphic arrangements and groundwater conditions were also identified from interpretation of site investigations located along alignments No. 1 and No. 2, although a certain horizontal spatial variability, in terms of both thickness and fine content of soil units *R* and *B* was observed. For this reason, the geotechnical model discussed in this study is specifically pertinent to section No. 3 (i.e. the closest alignment to the collapsed river embankment segment), whereas the geotechnical models of the other sections will not be presented because out of scope.

Accordingly, the geotechnical characterization of the different soil units relied on CPTU and SCPTU carried out in section No. 3, by applying semi-empirical correlations to field data. Results from laboratory tests were used as reference in order to validate the estimates of the mechanical parameters from in situ testing. The comparison between laboratory and field test results was mainly restricted to sediments forming the river embankment, since most of the samples were recovered in the upper 6 m. Furthermore, in view of the probabilistic analyses described in next sections, attention was primarily focused on the evaluation of the effective shear strength of the soil units. In particular, following previous successful experiences on natural silty mixtures referable to a very similar depositional environment of the Po river basin [40], the drained shear strength of *Unit R* and *Unit B*, expressed in terms of the effective friction angle at peak $\varphi'$, was determined using the well-established correlation proposed by Kulhawy and Mayne [41]. As regards the fine-grained *Unit C*, the estimates of $\varphi'$ were instead obtained from an effective stress limit plasticity solution [42] whose effectiveness was proved on a large database of natural clays [43]. This approach is based on the assumption that the effective cohesion intercept $c'$ is equal to 0, as reasonable in normally consolidated clays like those of *Unit C*.

Figure 3e shows estimates of $\varphi'$ obtained from SCPTU7. The resulting profile exhibits an initial decreasing trend in the upper portion of *Unit R*, referable to a sort of thin “crust” typically detected by cone penetration or dilatometer tests in the topmost soil layers of the Po river basin embankments (e.g. [40,44]) and likely due to overconsolidation for desiccation-wetting cycles together with partial saturation effects. As a results, the values of $\varphi'$ computed in this shallow thin lense were not considered as representative of *Unit R* and thus excluded from the statistical analysis presented herein.

Table 1 provides a summary of the statistical parameters computed for the effective shear strength of the different soil units, as obtained from the combined interpretation of SCPTU7, CPTU8 and CPTU9. The skewness of $\varphi'$ was always set equal to zero, as a consequence of the virtually symmetrical data distribution. It is worth observing that the range obtained for $\varphi'$ in *Unit R* (32°±1.9°) is fully consistent with the values (31.1°-34°) provided by triaxial tests, whereas in *Unit B* the effective friction angle from a few laboratory tests turned out to be close to the upper boundary identified by the statistical moments of Table 1. Unfortunately, laboratory test results in shearing were not available for *Unit C*, thus preventing any comparison between estimates of $\varphi'$. It is also interesting to notice that the values presented in Table 1 are consistent with those reported in the study of Phoon and Kulhawy [45], which was based on an extensive literature review.

Finally, it must be mentioned that the uncertainties on $\varphi'$ shown above do not include the so-called "transformation model" uncertainty, the attention being here primarily focused on the variability of the mechanical (and hydraulic) parameters as a consequence of the inherent heterogeneity of the investigated sediments. Nevertheless, it is worth emphasizing that, according to the recent study of Ching et al. [46], the CPT-$\varphi'$ transformation model [41] adopted in the present work for *Unit R* and *Unit B* was found to be nearly unbiased and with a broad application range.

| **Soil type** | **Friction angle $\varphi'$ (°)** mean value | standard deviation | skewness |
|---|---|---|---|
| *Unit_R* | 32.0 | 1.90 | 0 |
| *Unit_B* | 28.8 | 3.20 | 0 |
| *Unit_C* | 24.9 | 2.40 | 0 |

Table 1 – Statistical parameters (mean, standard deviation and skewness) of the friction angle **φ'**, for *Unit R*, *Unit B* and *Unit C*.

## 3.2 Unsaturated soil properties from evaporation tests

In order to characterize the soils forming the river embankment with respect to their hydraulic and retention response, series of evaporation tests were performed on nine undisturbed samples purposely collected near Section No. 3, at depths between 0.7 m and 1.7 m from the crest. Attention was obviously focused on sediments of the river embankment top layer *Unit R*, where unsaturated conditions are likely to apply. All tests were performed according to the procedure proposed by Romano and Santini [47], which relies on a parameter optimization strategy for the determination of unsaturated soil properties using evaporation data. In this study, the well-known and widely-used hydraulic model proposed by van Genuchten [48] was adopted to fit the experimental data; thus, hysteresis in the typical water retention behaviour of unsaturated soils was disregarded for the prediction of the effective degree of saturation, $S_e$. Accordingly, this can be determined as follows:

(11) $$S_e(h) = \frac{\theta-\theta_r}{\theta_0-\theta_r} = \left[\frac{1}{1+(\alpha_{VG}\cdot s)^{n_{VG}}}\right]^{m_{VG}}$$

where $\theta$, $\theta_0$ and $\theta_r$ are the volumetric soil water content at the current stage, at saturation and in residual conditions respectively, $s$ is the soil suction, given by the difference between the pore air pressure, $u_a$, and the pore water pressure, $u_w$, whilst $\alpha_{VG}$ and $n_{VG}$ are model parameters, mainly influencing the inflection and the shape of the retention curve respectively. Some authors [49] also refer to $\alpha_{VG}$ as the inverse of suction value at which the soil starts to desaturate. It is useful to remind that $n_{VG}$ and $m_{VG}$ are usually considered as inter-dependent parameters, defined as:

(12) $$m_{VG} = 1 - \frac{1}{n_{VG}}$$

In accordance with the Mualem's [50] model coupled with the parametrisation procedure suggested by van Genuchten [48], the variation of soil permeability with suction was derived from the Soil Water Retention Curve (SWRC), which describes the relationship between volumetric water content and matric suction. Hence, the following equation was used:

(13) $$k_r = S_e{}^{0.5}\left[1-\left(1-S_e{}^{1/m}\right)^m\right]^2$$

The above equation, typically referred to as Hydraulic Conductivity Function, defines the relationship between the effective degree of saturation, $S_e$, and the relative permeability, $k_r$. The hydraulic permeability of the soil is then obtained as the product of the saturated permeability, $k_0$, and the relative permeability, $k_r$.

Figure 5 shows the SWRCs obtained by fitting the available laboratory data using eq.(11). The plot provides the effective degree of saturation $S_e$ as a function of suction $s$. Although all the samples were taken from the same soil unit, a significant degree of heterogeneity is observed on the hydraulic behaviour of the soil in partially saturated conditions.

Based on such experimental results, a statistical interpretation of the hydraulic parameters of *Unit R*, expressed in terms of mean values, standard deviation, skewness and correlation structure, was carried out. It is worth observing that the amount of available laboratory test results can be considered as statistically significant for the proposed study, also considering that each evaporation test involved three independent measurements and that, at the same time, such dataset is significantly larger than those typically available in engineering practice. The computed mean values of the unsaturated hydraulic parameters of *Unit R*, together with standard deviation and skewness are listed in Table 2, whilst the relevant correlation matrix is provided in Table 3. The parameter $m_{VG}$ was obviously excluded from the list of hydraulic input variables, being dependent on $n_{VG}$.

| | Hydraulic parameters of *Unit R* | | |
|---|---|---|---|
| | mean value | standard deviation | skewness |
| $\theta_r$ [m$^3$/m$^3$] | 0.079 | 0.078 | 0.542 |
| $\theta_{sat}$ [m$^3$/m$^3$] | 0.395 | 0.041 | 0.026 |
| $\alpha_{VG}$ [kPa$^{-1}$] | 0.164 | 0.064 | -0.824 |
| $n_{VG}$ [-] | 1.328 | 0.154 | 0.016 |
| log ($k_0$) [log(m/s)] | -5.805 | 0.776 | -0.632 |

Table 2 – Statistical moments (mean, standard deviation and skewness) of the unsaturated hydraulic parameters of soil *Unit R*.

| | $\boldsymbol{\theta_r}$ m$^3$/m$^3$ | $\boldsymbol{\theta_{sat}}$ m$^3$/m$^3$ | $\boldsymbol{\alpha_{VG}}$ kPa$^{-1}$ | $\boldsymbol{n_{VG}}$ - | **log($k_0$)** log(m/s) |
|---|---|---|---|---|---|
| $\boldsymbol{\theta_r}$ | 1 | 0.0 | 0.0 | 0.37 | -0.51 |
| $\boldsymbol{\theta_{sat}}$ | - | 1 | 0.34 | 0.69 | 0.63 |
| $\boldsymbol{\alpha_{VG}}$ | - | - | 1 | –0.09 | 0.68 |
| $\boldsymbol{n_{VG}}$ | - | - | - | 1 | 0.23 |
| **log($k_0$)** | - | - | - | - | 1 |

Table 3 – Correlation matrix of the unsaturated hydraulic properties of soil *Unit R*.

It is worth mentioning that the statistical moments shown in Table 2 fall in the ranges typically reported in the literature. Indeed, according to a number of studies (e.g. [20,51-52]), based on either direct or indirect methods for the assessment of hydraulic parameters, typical ranges of the coefficient of variation ($CoV_{(X)} = \sigma_X/\mu_X$) of the Van Genuchten – Mualem model parameters are: $CoV_{(\theta_r)}$= 10-110%, $CoV_{(\theta_{sat})}$ = 5-25%, $CoV_{(\alpha_{VG})}$ = 20-100%, $CoV_{(n_{VG})}$ = 3-20%, $CoV_{(k_0)}$ = 100-300%. Besides, the mean values of Table 2 turn out to be fully consistent with those reported by Santoso et al. [53]. Regarding *Unit B* and *Unit C*, only the permeability at saturation, $k_0$, was taken into account, since both units are permanently below the phreatic line. Mean values of the permeability, as obtained from the application of empirical correlations to piezocone data [54], turn out to be $1.88 \cdot 10^{-6}$ m/s and $1.30 \cdot 10^{-9}$ m/s for *Unit B* and *Unit C,* respectively. It must be emphasized that the permeability of both units was considered as a deterministic parameter in the probabilistic analyses proposed herein.

# 4. Development of the seepage model for the stability analyses in transient conditions

The seepage and stability analyses were carried out with reference to a 2D river embankment model based on the geometry, stratigraphic conditions, geotechnical and hydrological data of section No. 3 of the river Secchia (Figure 4), as it used to be prior to failure, i.e. 7 m high, with the outer and inner slope angles equal to 30° and 33° respectively. In order to properly assess the stability of an existing river embankment with respect to a specific flooding event, it is necessary to undertake transient seepage analyses, accounting for both river level fluctuations and rainfall infiltration, starting from realistic initial conditions. Accordingly, the soil forming the river embankment, namely soil Unit *R* in this study, must be assumed as partially saturated, with relevant implications on both the seepage process and soil shear strength that will be discussed later. In particular, in the absence of specific measurements for the studied river embankment segment, a suitable initial suction distribution into the bank, which might be considered as typical during a period of significant rainfall events, was firstly sought. Following previous experiences of other Authors (e.g. [1,55-58]), the distribution eventually adopted assumes that suction is maximum in the river embankment core and approximately equal to zero at the free surface.

As a result, taking the water table at 30 m above the means sea level (m.s.l.), close to the transition surface between *Unit R* and *Unit B* (see Fig. 4), suction was assumed to linearly increase up to 39 kPa in correspondence of the centre of the bank, at 4 meters above the phreatic line, and then to decrease to zero close to the bank crest.

Flow through an earthen structure highly depends on the relative permeability of the fill material, which in turn depends on its degree of saturation. The transient unsaturated-saturated flow was modelled using the 2D Finite Element code SEEP/W [59], assuming the effective degree of saturation and the relevant hydraulic permeability derived from the application of the van Genuchten-Mualem model [48], as discussed in §3.2. The FE numerical solution is based on the Generalized Darcy Law for transient seepage conditions, given by:

(14) $$\boldsymbol{q} = \frac{\partial \theta}{\partial t} - k_r k_0 \nabla \left( \frac{u_w}{\gamma_w} + z \right)$$

where $z$ is the vertical elevation and $\boldsymbol{q}$ is the boundary flux per unit area. When the water storage in the model does not vary with time, steady-state conditions apply, basically corresponding to significantly high persistency of the hydrometric peak.

Positive and negative pore water pressure distributions obtained at the end of the seepage analysis were then imported into the code SLOPE/W [60] and assumed as input data for the riverbank stability calculations, using limit equilibrium methods. Among the different available approaches, the Morgenstern and Price [61] method was eventually selected to perform the stability analyses in transient flow conditions.

Slip surfaces were generated randomly, according to suitable pre-defined geometrical constraints, consisting in the ranges for the entry zone and the exit zone of the sliding mechanism on the ground surface, together with the so-called “minimum depth” (corresponding to the minimum height of

LEM slices). In this way, a significant collapse mechanism could be identified, while excluding potential local shallow slip surfaces (see Fig. 6). The minimum slip surface depth was assumed to be 1.5 m and 3.8 m for the inner and outer instability mechanisms, respectively. Furthermore, the potential slip surfaces were all circular, as actually observed in the collapse occurred in January 2014.

Regarding soil shear strength, the limit equilibrium analyses performed in this study made use of the Vanapalli et al. [62] failure criterion, which is implemented in SLOPE/W. As many other strength criteria for unsaturated soils, this approach derives from the linear shear strength equation originally proposed by Fredlund et al. [63], extending such formulation to account for the impact of non-linearity of the soil water retention curve on the resulting shear strength relationship. As a result, the shear strength of an unsaturated soil is assumed to vary with the degree of saturation ($S_e$) and the matric suction ($u_a - u_w$), according to the following expression:

(15) $$\tau = c' + (\sigma_n - u_a)tan\varphi' + (u_a - u_w)S_e tan\varphi'$$

with $\sigma_n$ = the total normal stress, $c'$ = effective cohesion, $\varphi'$ = effective stress friction angle.

The first part of the equation describes the saturated shear strength, which is a function only of the normal stress since the shear strength parameters $c'$ and $\varphi'$ are assumed as constant for a saturated soil. The second part [i.e., $(u_a - u_w)\cdot S_e \cdot tan\varphi'$] provides the shear strength contribution due to suction, which can be predicted using the soil water retention curve [64]. In particular, the formulation described by eq.(15) fulfils a number of well-known experimental evidences reported by various Authors (e.g. [62,65]): when the soil begins to desaturate, the unsaturated soil strength contribution varies according to a non-linear function of suction, as long as the matric suction remains above the air entry value (AEV), this latter corresponding to the point at which air enters the largest pores of the soil [50]. By contrast, when suction is below AEV, the unsaturated shear strength is equal to $(u_a - u_w)\cdot\tan\varphi'$. In saturated conditions, when the pore-air pressure, $u_a$, is equal to the pore-water pressure, $u_w$, eq. (15) turns into the classical Mohr – Coulomb failure criterion.

With respect to the shear strength values adopted in the analyses, a few points must be emphasized. First of all, it is worth remarking that the use of data only from the evaporation tests prevented from dealing with soil hysteresis in the water retention behaviour. As a matter of fact, the seepage process to be modelled in this study is not truly referable to wetting paths, but rather to scanning paths, which in turn would require specific laboratory tests for characterization. On the other hand, a few preliminary analyses based on the parameters estimated for the wetting branch, according to suggestions of Likos et al. [52], showed that the use of data from a main drying curve generally does not provide results on the unsafe side in terms of reliability assessment, which is indeed the main focus of this study. This outcome is due to a combination of different governing factors that result in opposite effects on the numerical assessment of the riverbank stability and the prevalence of one effect on the others should be analysed in each specific case. Indeed, although the assumption of non-hysteretic hydraulic behaviour might tend to overestimate the suction values for an assigned effective degree of saturation, the relative permeability would be then underestimated by the van Genuchten model, with evident consequences on the flow regime and leading, at the end of high water events, to a minor impact on the phreatic line, particularly when initial conditions are defined in terms of suction.

# 5. Probabilistic stability analysis

The probabilistic analysis of the riverbank stability was organized into two main stages, referred to as "First-level probabilistic analysis" and "Second-level probabilistic analysis" respectively. The first includes a few preliminary analyses based on the assumption that the soil friction angle φ' is the only random variable. Both steady-state seepage conditions, typically suggested by guidelines, and transient seepage in partially saturated soils, were modelled. Indeed, although the steady-state seepage turns out to be the most critical situation for the stability of a river embankment, only a transient seepage approach, accounting for fluctuations of the river water level and rainfall infiltration, can realistically identify the actual margins of safety of the structure during a specific flooding event. Obviously, the variability of the friction angle has no effects on the finite element seepage analysis, thus only affecting slope stability results.

By contrast, in the "Second-level probabilistic analysis", the riverbank reliability analysis was carried out solely under transient seepage conditions, accounting for uncertainties in both the effective friction angle and the unsaturated soil hydraulic parameters. In this way, the different impact produced by different sources of uncertainties in soil parameters may be identified.

At this point, it must be observed that a comprehensive stochastic analysis of the seepage through the river embankment should also consider the aleatory uncertainty associated with the initial pore water pressure distribution [66], which in turn depends on the river water level fluctuations. In this study, however, such aspect was disregarded, being the attention basically focused on the variability of geotechnical parameters and its effects on the riverbank reliability.

## 5.1 First-level probabilistic analysis

### *5.1.1 Steady state conditions*

The steady state seepage analysis was performed assuming the river level at the maximum hydrometric height recorded during the January 2014 flooding event, i.e. at 35.9 m above mean sea level [21], whilst the water table on landward side was located at the ground level. Constant values of the hydraulic conductivities were adopted for the different soil units, namely equal to the saturated permeability $k_0$ reported in Table 2 for *Unit R* and to the values of $k_0$ mentioned in § 3.2 for *Unit B* and *Unit C*. Figure 7 shows the computed pore water pressure (PWP) and the corresponding pressure head distributions, used in turn as input for the limit equilibrium analyses. The latter are based on the assumption that the soil shear strength obeys the effective stress Mohr-Coulomb failure criterion and that the friction angle of the river embankment soil unit (*Unit R*) follows a normal distribution, described by the statistical moments reported in Table 1 (mean shear strength = 32.0°, standard deviation = 1.9°). In these analyses, the contribution to shear strength due to suction is disregarded. The shear strength parameters of the underlying soil units, i.e. *Unit B* and *Unit C,* were considered as deterministic variables, the main goal being to investigate the effect of soil strength variability only within the river embankment. In this case, the model uncertainty is described by just one random variable and therefore the application of the *Point Estimate Method* requires only two combinations. For each point estimate combination, the most critical slip surface, in terms of safety factor, was randomly searched.

As mentioned in §2, these preliminary analyses were performed using both PEM and MCM, in order to assess the accuracy of the probability of failure provided by the *Point Estimate Method* compared to results of the robust *Monte Carlo* approach, the latter requiring a relatively moderate computational effort when uncertainty in soil parameters is limited to a single random variable. Values of the safety factor and probability of failure obtained from the probabilistic analyses are summarized in Table 4. A substantial agreement between the MCM and PEM results can be observed in this case, thus providing support for the application of only the *Point Estimate Method* to the whole stability problem discussed in this paper. Agreement between the two probabilistic methods was also documented by Vannucchi [67] with respect to other geotechnical applications.

Probabilistic Analysis Results – Steady state seepage conditions – PEM and MCM

| Safety Factor | Outer slope | | Inner slope | |
|---|---|---|---|---|
| | PEM | MCM | PEM | MCM |
| Mean ($\mu_{SF}$) | 1.013 | 1.013 | 1.405 | 1.405 |
| Standard deviation ($\sigma_{SF}$) | 0.046 | 0.047 | 0.106 | 0.107 |
| Reliability index ( $\beta_{SF}$) | 0.283 | 0.274 | 3.821 | 3.791 |
| Probability of failure (%) | 38.9 | 39.9 | $6.7 \cdot 10^{-3}$ | $7.3 \cdot 10^{-3}$ |

Table 4 – Probabilistic results of limit equilibrium analyses in steady state condition, for outer and inner slopes, with deterministic soil bank hydraulic parameters.

It is worth observing that the stability analyses in steady seepage conditions, though not representative for the specific flooding event, provide a sort of reference benchmark and useful information with regard to the existing margin of safety of the river embankment. Indeed, according to the computed values of the reliability index $\beta_{SF}$, which turn out to be very low, the stability of the outer slope in case of persistent high river water levels appears critical. By contrast, a high reliability index value (thus implying a low probability of failure) was obtained for the most critical surface of the inner slope.

#### *5.1.2 Transient seepage conditions*

In transient seepage analyses, the river water level fluctuation was modelled as time-dependent boundary condition on the riverside FE mesh nodes, expressed in term of total hydraulic head. Rainfall infiltration was simulated as water flux through the boundary surface, based on the hydrometric values and precipitation data recorded in close proximity to the investigated breached area, from 25 December 2013 to the flooding event date (19 January 2014). The daily river levels and rainfall recorded by the competent Regional Authority are plotted in Figure 8, together with the approximated profile of the total hydraulic head variation versus time, applied at the riverside boundary of the numerical model. Figure 9 shows the computed pore water pressure distributions at the initial and final stage of transient seepage analysis. As regards the unsaturated hydraulic parameters of *Unit R*, here treated as deterministic variables, the mean values of Table 2 were adopted.

The subsequent probabilistic limit equilibrium analysis, based on the PEM approach, resulted in very high values of the reliability index $\beta_{SF}$ (i.e. very low probabilities of failure), especially for the inner slope (Table 5). Since the probability of failure provided by PEM may suffer from a lack of accuracy at very small probability levels, in this study a threshold value equal to $10^{-3}$% was assumed as reference for the minimum value of $P_f$, hence the reason for $P_f$ expressed as $<10^{-3}$% in

Table 5. On the other hand, probabilities of failure lower than $10^{-3}$% does not seem to provide additional information with respect to the riverbank stability conditions.

| Probabilistic Analysis Results – Transient seepage conditions | | |
|---|---|---|
| Safety Factor | Outer slope | Inner slope |
| Mean ($\mu_{SF}$) | 1.346 | 2.077 |
| Standard deviation ($\sigma_{SF}$) | 0.063 | 0.156 |
| Reliability index ( $\beta_{SF}$) | 5.492 | 6.904 |
| Probability of failure ($P_f$, %) | < $10^{-3}$ | < $10^{-3}$ |

Table 5 – Probabilistic results of M-P limit equilibrium analyses in transient seepage condition, for outer and inner slopes, with deterministic soil bank hydraulic parameters.

## 5.2 Second-level probabilistic analysis

The second-level probabilistic analysis was performed in order to investigate the effect of multiple sources of uncertainties in soil parameters (i.e. both shear strength and unsaturated hydraulic properties) on the assessment of riverbank stability, expressed in terms of the degree of uncertainty associated with the safety factor.

For this purpose, three different sets of probabilistic analyses were devised, according to the different assumptions adopted in the cases specified below:

*Case 1*: friction angle ($\varphi'$) of *Unit R* assumed as random variable and hydraulic parameters ($\vartheta_r$, $\vartheta_0$, $\alpha_{VG}$, $n_{VG}$, $k_0$) as deterministic variables, equal to their mean values.

*Case 2*: shear strength angle ($\varphi'$) and hydraulic parameters ($\vartheta_r$, $\vartheta_0$, $\alpha_{VG}$, $n_{VG}$, $k_0$) of *Unit R* assumed as non-correlated random variables.

*Case 3*: shear strength angle ($\varphi'$) and hydraulic parameters ($\vartheta_r$, $\vartheta_0$, $\alpha_{VG}$, $n_{VG}$, $k_0$) of *Unit R* assumed as correlated random variables.

As a matter of fact, *Case 1* corresponds to the first-level probabilistic analysis in transient seepage condition commented in § 5.1.2.

The remaining two cases were analysed following the methodological approach already described, i.e. transient seepage analyses were carried out using appropriate hydraulic soil parameters and then, based on the computed pore water pressure distributions, for each point estimate combination the most critical slip surface was randomly searched. Hence, such analyses are not based on a deterministic choice of a predefined critical failure surface, which therefore may vary as different point estimate combinations are adopted. In both *Case 2* and *Case 3*, probabilistic analyses considered a total of 6 random variables: the friction angle $\varphi'$ and 5 hydraulic parameters ($\theta_r$, $\theta_{sat}$, $\alpha_{VG}$, $n_{VG}$, $k_0$) of *Unit R*. In this way, the application of PEM resulted in 64 combinations of point estimate locations. Histograms of each random variable, together with the indication of the point estimate locations ($X_+$ and $X_-$) and the associated weights ($P_+$ and $P_-$), are shown in Figure 10.

The method consists in calculating the safety factor *SF* for each set of parameters in a deterministic way. According to the procedure described in § 2.1, results were then suitably processed in order to obtain the mean $\mu_{SF}$ and the standard deviation $\sigma_{SF}$ of safety factor *SF*, assumed as a normally distributed random variable.

# 6. Discussion of results

Results of the probabilistic analyses for the three cases investigated in the second-level probabilistic analysis are summarized in Figures 11 and 12, plotted in terms of probability density function (PDF) of the safety factor, cumulative density function (CDF) and probability of failure ($P_f$) associated with the safety factor, for both the outer and the inner riverbank slopes. It is worth mentioning here that the probability of failure can be easily determined from the cumulative density function for a safety factor equal to 1 ($CDF_{SF=1}$), since $P_f$ (%) = 100 x $CDF_{SF=1}$.

Figure 11 clearly shows that the mean value of the safety factor is approximately equal to 1.3 for the outer slope and close to 2.0 for the inner slope, with minor differences among the three cases mentioned above. Hence, the riverside zone appears to be significantly more stable than the landward zone. In general, it is immediate to observe that for this case study standard safety factors are sufficiently high; in fact, with regards to the most probable causes of the sudden collapse occurred in January 2014, other possible local structural weaknesses – like the extensive presence of animal burrows – were eventually advocated having triggered the catastrophic event [21]. However, this probabilistic study allows identifying very significant differences in the evaluation of the riverbank reliability, as a consequence of the different assumptions adopted in the three series of numerical analyses, which deserve particular attention in the light of common risk assessment procedures. In *Case 2* and *Case 3*, both accounting for the variability of hydraulic parameters in addition to shear strength, the uncertainty degree in the estimate of the safety factor increases considerably, with associated rather low values of the reliability index $\beta$, always lower than 3.5. Accordingly, the probability of failure turns out to be non-negligible, namely higher that $10^{-2}$% for both the inner and outer slope, whilst extremely low values of $P_f$ (< $10^{-3}$ %) were obtained when the only source of uncertainty was assumed to lie in shear strength (*Case 1*).

In particular, the probability density functions plotted in Figure 11 provide clear evidence of an increase in the standard deviation of the safety factor when the stability analyses are carried out under stochastic unsaturated transient seepage conditions. The effect may be appreciated in both riverbank slopes, although it is undoubtedly more noticeable for the riverside stability analyses, being the shape of the probability distributions associated with *Case 2* and *Case 3* significantly wider than the “thin” shape of *Case 1*.

Besides, the probability of failure provided by the numerical analyses of *Case* 3, reflecting the uncertainties of the unsaturated hydraulic parameters as well as their correlation structure, is one order of magnitude smaller than that obtained in *Case* 2, the latter being based on the assumption of no correlation between the parameters. Such outcome is consistent with results reported by Zhang et al. [68-69] with respect to slope stability problems. Indeed, additional information on the input parameters result in a better knowledge of them, thus leading to a reduction of the degree of uncertainty. This point was extensively discussed also by Phoon et al. [20], who observed that correlations between unsaturated hydraulic parameters should be investigated as a preliminary step in any probabilistic study instead of assuming a priori their independence for expediency.

Furthermore, Figure 13 shows results of a sensitivity analysis on the input parameters, i.e. shear strength and hydraulic parameters, aimed at investigating their relative importance on the river embankment response. Such relative contribution was quantified in terms of the variance of the safety factor, $\sigma_{SF}^2$, defined according to eq.(8). In particular, the contribution of the hydraulic parameters to $\sigma_{SF}^2$ was simply evaluated as the difference between the safety factor variance computed in *Case 2* ($\sigma_{SF,c2}^2$) or, alternatively, in *Case 3* ($\sigma_{SF,c3}^2$) and the safety factor variance associated with *Case 1* ($\sigma_{SF,c1}^2$), the latter being based on the uncertainty in shear strength (φ') only. Accordingly, for *Case 2* and *Case 3*, the per cent relative contribution of the effective friction angle ($\sigma_{\%,\varphi'}^2$) and the hydraulic parameters ($\sigma_{\%,hp}^2$) to the safety factor variance can be evaluated as follows:

(16a) $\sigma^2_{\%,\varphi'} = 100 \cdot \sigma^2_{SF,c1}/\sigma^2_{SF,c2}$ *Case 2*

or

(16b) $\sigma^2_{\%,\varphi'} = 100 \cdot \sigma^2_{SF,c1}/\sigma^2_{SF,c3}$ *Case 3*

(17a) $\sigma^2_{\%,hp} = 100 \cdot \left(\sigma^2_{SF,c2} - \sigma^2_{SF,c1}\right)/\sigma^2_{SF,c2}$ *Case 2*

or

(17b) $\sigma^2_{\%,hp} = 100 \cdot \left(\sigma^2_{SF,c3} - \sigma^2_{SF,c1}\right)/\sigma^2_{SF,c3}$ *Case 3*

According to results plotted in Figure 13, the unsaturated hydraulic parameters appear to have the largest influence on the uncertainty of the safety factor, with percentages of contribution in the ranges 72-84% and 79-83% for the outer slope and inner slope respectively.

A final parametric study was undertaken in order to gain a better insight into the effect of the coefficient of variation of the only friction angle φ', $CoV_{(\varphi')}$, on the probability of failure, with respect to both riverbank slopes. For this purpose, three different values of $CoV_{(\varphi')}$, selected within the typical interval (i.e. 5-15%) quoted for this statistical parameter by various authors (e.g. [3,45,70,71]), were investigated, while assuming the unsaturated hydraulic properties either as deterministic or correlated random variables. Results of these series of analyses, expressed in terms of probability of failure versus $CoV_{(\varphi')}$, are plotted in Figure 14. For $CoV_{(\varphi')} = 6\%$, corresponding to the value computed from the available experimental estimates, the values of $P_f$ coincide with those previously calculated in *Case 1* (i.e. deterministic transient seepage) and *Case 3* (i.e. stochastic transient seepage based on correlated hydraulic random variables).

As the coefficient of variation of the shear strength increases from 6% to 15%, the impact of $\varphi'$ on the variance of the safety factor was found to consistently increase, causing in turn a decrease in the relative importance of the hydraulic parameters on the output. However, Figure 14 clearly shows that the difference between the probability of failure obtained under the opposite hypotheses of stochastic and deterministic transient seepage remains significant as long as $CoV_{(\varphi')}$ does not exceed 10% for the outer riverbank slope and 15% for the inner slope.

This outcome demonstrates that for usual values of uncertainty degree of the effective friction angle, the variability of the unsaturated soil hydraulic parameters plays a crucial role in the assessment of the probability of failure of the riverbank slopes. Hence, neglecting the intrinsic variability of such parameters, even in soils assumed as relatively homogenous from a geotechnical point of view, may lead to estimates of the probability of failure which are not consistent with the real risk and typically non conservative. Further investigations and additional datasets from specific case studies are obviously required in order to confirm the above results and draw more comprehensive conclusions.

# 7. Conclusions

This paper has presented a probabilistic study aimed at exploring the role of partial saturation of soils and of intrinsic variability of the relevant hydraulic parameters, beside shear strength, on the stability of existing river embankments. The issue has been discussed with reference to actual data of a specific 20m-long stretch of the river Secchia banks (northern Italy), which was extensively investigated following its catastrophic sudden collapse occurred in January 2014, after a period of intense rainfall. The large and varied geotechnical database related to this case study has enabled the development of a detailed geotechnical model of the breached segment, inclusive of the mechanical and hydraulic behaviour of the sediments forming the unsaturated river embankment, thus allowing sound probabilistic analyses supported by experimental results.

Uncertainties on geotechnical data are typically disregarded in standard practice and only a very limited number of research contributions have considered the effect of the variability of hydraulic soil properties on riverbank stability. Furthermore, according to recommendations of current geotechnical codes and standards, the assessment of riverbank stability is generally based on the over-simplified assumption of steady state seepage in equilibrium with the highest possible river level.

In this study, three key features have been taken into consideration: 1) the time-dependent hydraulic boundary conditions due to water level fluctuations in the river, thus requiring a transient seepage analysis; 2) the unsaturated initial state of the river embankment; 3) the uncertainty in the geotechnical parameters, including those describing the unsaturated behaviour of sediments.

The probabilistic analyses have been carried out using the Point Estimate Method, a widely recognized procedure for slope reliability analyses, which appears to offer significant advantages in terms of efficiency over the more robust Monte Carlo method where the assessment of the probability of failure can be computationally intensive.

The reason for adopting this simplified uncertainty propagation method is twofold. Infact, apart from its efficiency and rather straightforward implementation procedure, which make the approach attractive for use also in routine risk analyses, the idea behind the study is basically to explore the relative weight of a number of random variables on the stability assessment of a river embankment, expressed in terms of probability of failure.

Although the actual safety factors of both inner and outer slopes of the Secchia river embankment are generally far from unity, thus suggesting that the January 2014 failure should be most likely seen as due to lack of local integrity for animal burrows, the results presented in this paper have proved that the probability of failure is strongly influenced by the suction distribution, which in turn depends on the hydraulic parameters adopted in the analyses. When uncertainty in unsaturated hydraulic parameters is taken into account, the probability of failure turns out to be significantly higher than that obtained on the assumption that shear strength is the only random variable, the difference being in this case of various orders of magnitude. This study has also shown that for the usual uncertainty degree of shear strength, the variability of the unsaturated soil hydraulic parameters has a major impact on the resulting probability of failure, for both riverbank slopes. Hence, not only the unsaturated transient seepage conditions are of outmost importance in the assessment of riverbank stability, but also underestimating the effect of the intrinsic variability of hydraulic parameters, even in soils assumed as relatively homogenous, may lead to probabilities of failure which are not consistent with the actual risk and potentially non-conservative. The latter aspect, which is typically neglected in routine risk assessment procedures either for lack of relevant experimental data or lack of awareness of the potential consequences, should be taken in careful consideration instead.

Further investigations and additional datasets from specific case studies would be required in order to confirm the results discussed in this study and draw more comprehensive conclusions. It is finally worth observing that, in spite of a certain roughness, the Point Estimate Method has proved to clearly capture the effect of the intrinsic variability of the unsaturated soil hydraulic properties on the reliability analysis of the river embankment.

# References

[1] Rinaldi M, Casagli N, Dapporto S, Gargini A. Monitoring and modelling of pore water

pressure changes and riverbank stability during flow events. Earth Surf Process Landforms 2004;29(2):237–54. doi:10.1002/esp.1042.

[2] Liang C, Jaksa MB, Ostendorf B, Kuo YL. Influence of river level fluctuations and climate on riverbank stability. Comput Geotech 2015;63:83–98. doi:10.1016/j.compgeo.2014.08.012.

[3] Baecher GB, Christian JT. Reliability and Statistics in Geotechnical Engineering. 2003.

[4] Ching J, Phoon KK. Establishment of generic transformations for geotechnical design parameters. Struct Saf 2012;35:52–62. doi:10.1016/j.strusafe.2011.12.003.

[5] Low BK. FORM, SORM, and spatial modeling in geotechnical engineering. Struct Saf 2014;49:56–64. doi:10.1016/j.strusafe.2013.08.008.

[6] Aguilar-López JP, Warmink JJ, Schielen RMJ, Hulscher SJMH. Soil stochastic parameter correlation impact in the piping erosion failure estimation of riverine flood defences. Struct Saf 2016;60:117–29. doi:10.1016/j.strusafe.2016.01.004.

[7] Zhao T, Montoya-Noguera S, Phoon K-K, Wang Y. Interpolating spatially varying soil property values from sparse data for facilitating characteristic value selection. Can Geotech J 2018;55:171–181. doi:10.1139/cgj-2017-0219.

[8] Zhang L, Li J, Li X, Zhang J, Zhu H. Rainfall-Induced Soil Slope Failure: Stability Analysis and Probabilistic Assessment. CRC Press, Taylor & Francis Ltd, London, United Kingdom, 2019.

[9] Christian BJT, Ladd CC, Baecher GB. Reliability Applied to Slope Stability Analysis. J Geotech Eng 1994;120(12):2180–207.

[10] Husein Malkawi AI, Hassan WF, Abdulla FA. Uncertainty and reliability analysis applied to slope stability. Struct Saf 2000;22:161–87. doi:10.1016/S0167-4730(00)00006-0.

[11] Ranalli M, Medina-Cetina Z, Gottardi G, Nadim F. Probabilistic calibration of a dynamic model for predicting rainfall-controlled landslides. Journal of Geotechnical and Geoenvironmental Engineering 2014;140(4):4013039.

[12] Jiang SH, Huang JS. Efficient slope reliability analysis at low-probability levels in spatially

variable soils. Comput Geotech 2016;75:18–27. doi:10.1016/j.compgeo.2016.01.016.

[13] Zhang J, Huang HW, Zhang LM, Zhu HH, Shi B. Probabilistic prediction of rainfall-induced slope failure using a mechanics-based model. Engineering Geology 2014;168:129-40. doi:10.1016/j.enggeo.2013.11.005

[14] Santoso A, Phoon KK, Quek ST. Effects of soil spatial variability on rainfall-induced landslides. Computers and Structures 2011;89(11–12):893-900. doi:10.1016/j.compstruc.2011.02.016

[15] Tung YK, Chan GCC. Stochastic analysis of slope stability considering uncertainties of soil-water retention characteristics. In: Proceedings 9th Int. Conf. on Applications of Statistics and Probability in Civil Engineering; 2003. p. 1409–14.

[16] Zhang LL, Zhang LM, Tang WH. Rainfall-induced slope failure considering variability of soil properties. Géotechnique 2005;55(2):183–88.

[17] Liu K, Vardon PJ, Hicks MA, Arnold P. Combined effect of hysteresis and heterogeneity on the stability of an embankment under transient seepage. Eng Geol 2017;219:140–50.

[18] Cho SE. Probabilistic analysis of seepage that considers the spatial variability of permeability for an embankment on soil foundation. Eng Geol 2012;133–134:30–9.

[19] Le TMH, Gallipoli D, Sanchez M, Wheeler SJ. Stochastic analysis of unsaturated seepage through randomly heterogeneous earth embankments. Int J Numer Anal Methods Geomech 2012;36:1056–76. doi:10.1002/nag.1047.

[20] Phoon K-K, Santoso A, Quek S-T. Probabilistic Analysis of Soil-Water Characteristic Curves. J Geotech Geoenvironmental Eng 2010;136:445–55.

[21] D'Alpaos L, Brath A, Fioravante V. Relazione tecnico-scientifica sulle cause del collasso dell ' argine del fiume Secchia avvenuto il giorno 19 gennaio 2014 presso la frazione San Matteo. Http://AmbienteRegioneEmilia-RomagnaIt/Geologia/Notizie/Notizie-2014/Fiume-Secchia 2014.

[22] Wolff TF. Probabilistic slope stability in theory and practice. In: C.D. Shackelford PPN and

MJSR, editor. Uncertain. Geol. Environ., University of Wisconsin–Madison Press; 1996, p. 419–33.

[23] Duncan JM. Factors of Safety and Reliability in Geotechnical Engineering. J Geotech Geoenvironmental Eng 2000;126:307–16. doi:10.1061/(ASCE)1090-0241(2000)126:4(307).

[24] Vannucchi G, Gottardi G, Madiai C, Marchi M, Tonni L. Analisi della probabilità di collasso arginale dei grandi fiumi. Atti del XXV Convegno Naz. di Geotec., Baveno, Italy: 2014, p. 303–19.

[25] Ahmed A, Soubra AH. Probabilistic analysis at the serviceability limit state of two neighboring strip footings resting on a spatially random soil. Struct Saf 2014;49:2–9.

[26] Li D, ChenYF, Lu WB, Zhou CB. Stochastic response surface method for reliability analysis of rock slopes involving correlated non-normal variables. Computers and Geotecnics 2011;38(1):58-68.

[27] Au SK, Ching J, Beck JL. Application of subset simulation methods to reliability benchmark problems. Structural Safety 2007;29:183–93. doi:10.1016/j.strusafe.2006.07.008

[28] Li DQ, Xiao T, Cao ZJ, Zhou CB, Zhang LM. Enhancement of random finite element method in reliability analysis and risk assessment of soil slopes using Subset Simulation. Landslides 2016;13(2):293–303. doi:10.1007/s10346-015-0569-2

[29] Wang Z, Broccardo M, Song J. Hamiltonian Monte Carlo methods for Subset Simulation in reliability analysis. Structural Safety 2019;76:51–67. doi:10.1016/j.strusafe.2018.05.005

[30] Duncan JM, Sleep MD. Evaluating reliability in geotechnical engineering. In: Phoon K-K, Ching J, editors. Risk Reliab. Geotech. Eng., CRC Press; 2015, p. 50.

[31] Schweiger HF, Thurner R, Pöttler R. Reliability Analysis in Geotechnics with Deterministic Finite Elements. Int J Geomech 2001;1:389–413. Doi:10.1061/(ASCE)1532-3641(2001)1:4(389)

[32] Sekhavatian A, Janalizadeh Choobbasti A. Comparison of Point Estimate and Monte Carlo probabilistic methods in stability analysis of a deep excavation. International Journal of Geo-

Engineering 2018;9(1):20. doi:10.1186/s40703-018-0089-8

[33] Liyama K, Yoshiyuki A, Fujita K, Ichimura T, Morikawa H, Hori M. A point-estimate based method for soil amplification estimation using high resolution model under uncertainty of stratum boundary geometry. Soil Dynamics and Earthquake Engineering 2019;121:480-90.

[34] Rosenblueth E. Point estimates for probability moments. Proc Natl Acad Sci U S A 1975;72:3812–4. doi:10.1073/pnas.72.10.3812.

[35] Lind NC. Modelling of uncertainty in discrete dynamical systems. Appl Math Model 1983;7:146–52. doi:10.1016/0307-904X(83)90001-X.

[36] Harr ME. Probabilistic estimates for multivariate analyses. Appl Math Model 1989;13:313–8. doi:10.1016/0307-904X(89)90075-9.

[37] Panchalingam G, Harr ME. Modelling of many correlated and skewed random variables. Appl Math Model 1994;18:635–40. doi:10.1016/0307-904X(94)90322-0.

[38] Robertson PK. Interpretation of cone penetration tests — a unified approach. Can Geotech J 2009;46:1337–55. doi:10.1139/T09-065.

[39] Tonni L, Gottardi G. Interpretation of piezocone tests in Venetian silty soils and the issue of partial drainage. In: Deep foundations and geotechnical in situ testing, ASCE Geotechnical Special Publication No. 178. Reston (Virginia): ASCE; 2010. pp. 367-74.

[40] Tonni L, Gottardi G, Amoroso S, Bardotti R, Bonzi L, Chiaradonna A, D'Onofrio A, Fioravante V, Ghinelli A, Giretti D, Lanzo G, Madiai C, Marchi M, Martelli L, Monaco P, Porcino D, Razzano R, Rosselli S, Severi P, Silvestri F, Simeoni L, Vannucchi G, Aversa S. Interpreting the deformation phenomena triggered by the 2012 Emilia seismic sequence on the Canale Diversivo di Burana banks. Rivista Italiana di Geotecnica 2015;49(2):28-58.

[41] Kulhawy FH, Mayne PW. Manual on Estimating Soil Properties for Foundation Design. 1990.

[42] Mayne PW, Campanella RG. Versatile site characterization by seismic piezocone. 16th Int. Conf. Soil Mech. Geotech. Eng. 12-16 Sept. 2005, Osaka, Japan: 2005, p. 721–4.

[43] Ouyang Z, Mayne PW. Effective friction angle of clays and silts from piezocone penetration tests. Canadian Geotechnical Journal 2018;55:1230–47 doi:10.1139/cgj-2017-0451

[44] Gottardi G, Marchi M, Tonni L. Static stability of Po river banks on a wide area. In: Proc. 16th ECSMGE, 2015. p. 1675-80. doi:10.1680/ecsmge.60678

[45] Phoon K-K, Kulhawy FH. Characterization of geotechnical variability. Canadian Geotechnical Journal 1999;36:612–624.

[46] Ching J, Lin G-H, Chen J-R, Phoon K-K. Transformation models for effective friction angle and relative density calibrated based on generic database of coarse-grained soils. Canadian Geotechnical Journal 2017;54: 481–501. doi:10.1139/cgj-2016-0318

[47] Romano N, Santini A. Determining soil hydraulic functions from evaporation experiments by a parameter estimation approach: Experimental verifications and numerical studies. Water Resour Res 1999;35:3343–59. doi:10.1029/1999WR900155.

[48] van Genuchten MT. A Closed-form Equation for Predicting the Hydraulic Conductivity of Unsaturated Soils1. Soil Sci Soc Am J 1980;44:892.

[49] Olivella S, Gens A. Vapour transport in low permeability unsaturated soils with capillary effects. Transp Porous Media 2000;40:219–41. doi:10.1023/A:1006749505937.

[50] Mualem Y. A new model for predicting the hydraulic conductivity of unsaturated porous media. Water Resour Res 1976;12:513–22. doi:10.1029/wr012i003p00513.

[51] Schaap MG, Leij FJ, Van Genuchten MT. Neural network analysis for hierarchical prediction of soil hydraulic properties. Soil Sci Soc Am J 1998;62:847–55.

[52] Likos WJ, Lu N, Godt JW. Hysteresis and Uncertainty in Soil Water-Retention Curve Parameters. J Geotech Geoenvironmental Eng 2014;140:04013050.

[53] Santoso A, Phoon KK, Quek ST. Probability models for SWCC and hydraulic conductivity. In: Proceedings 14th Asian Regional Conference on Soil Mechanics and Geotechnical Engineering, Hong Kong, China, 23-27 May 2011.

[54] Robertson PK, Cabal KL. Guide to cone penetration testing for geotechnical engineering. In:

Gregg Drilling & Testing I, editor. 6th Edition, 2015, p. 133.

[55] Casagli N, Rinaldi M, Gargini A, Curini A. Pore water pressure and streambank stability: Results from a monitoring site on the Sieve River, Italy. Earth Surf Process Landforms 1999;24:1095–114.

[56] Calabresi G, Colleselli F, Danese D, Giani G, Mancuso C, Montrasio L, et al. Research study of the hydraulic behaviour of the Po River embankments. Can Geotech J 2013;50:947–60.

[57] Gragnano CG, Bertolini I, Rocchi I, Gottardi G. On the stability of a fully instrumented river embankment under transient conditions. In: Proceedings CNRIG 2019;40:369-378.

[58] Sleep MD, Duncan JM. Effects of initial conditions on the results of transient seepage analyses. In: ASCE, editor. Proc. Geo-Congress 2013 Stab. Perform. Slopes Embankments III, San Diego, California, US: 2013, p. 1081–91.

[59] GEO-SLOPE International Ltd. Seepage Modeling with SEEP/W; 2007. http://www.geo-slope.com.

[60] GEO-SLOPE International Ltd. Stability modeling with SLOPE/W; 2007. http://www.geo-slope.com.

[61] Morgenstern NR, Price VE. Analysis of the stability of general slip surfaces. Géotechnique 1965;15(1):79–93.

[62] Vanapalli SK, Fredlund DG, Pufahl DE, Clifton AW. Model for the prediction of shear strength with respect to soil suction. Can Geotech J 1996;33:379–92. doi:10.1139/t96-060.

[63] Fredlund DG, Morgenstern NR, Widger RA. The shear strength of unsaturated soils. Can Geotech J 1978;15:313–21. doi:10.1139/t78-029.

[64] Fredlund DG, Vanapalli SK. Shear strength of unsaturated soils. Agron Soil Test Man 2002:329–61.

[65] Lu N, Likos WJ. Unsaturated soil mechanics. New York: Wiley. 2004.

[66] Gottardi G, Gragnano CG. On the role of partially saturated soil strength in the stability analysis of a river embankment under steady-state and transient seepage conditions. E3S

Web Conf., vol. 9, 2016. doi:10.1051/e3sconf/20160919002.

[67] Vannucchi G. Analisi probabilistica speditiva in geotecnica e fondazioni. Riv Ital Di Geotec 1985;19:77–87.

[68] Zhang L, Zhang L, Tang W. Importance of considering correlations among parameters of soil-water characteristic curve. 9th Int. Conf. Appl. Stat. Probab. Civ. Eng., San Francisco, US: 2003, p. 1423–9.

[69] Zhang L, Deng H, Zhang L. Reliability analysis of slope stability considering correlations among soil hydraulic parameters. J Shenzhen Univ Sci Eng 2010;27:114–9.

[70] Lee I, White W, Ingles O. Geotechnical engineering. Boston, US: Pitman Publishing; 1983.

[71] Lacasse S, Nadim F. Uncertainties in characterising soil properties. Publ - Norges Geotek Inst 1996;201:49–75.

Figure

**Figure 1** – Images of the breached area during the River Secchia flooding in January 2014.

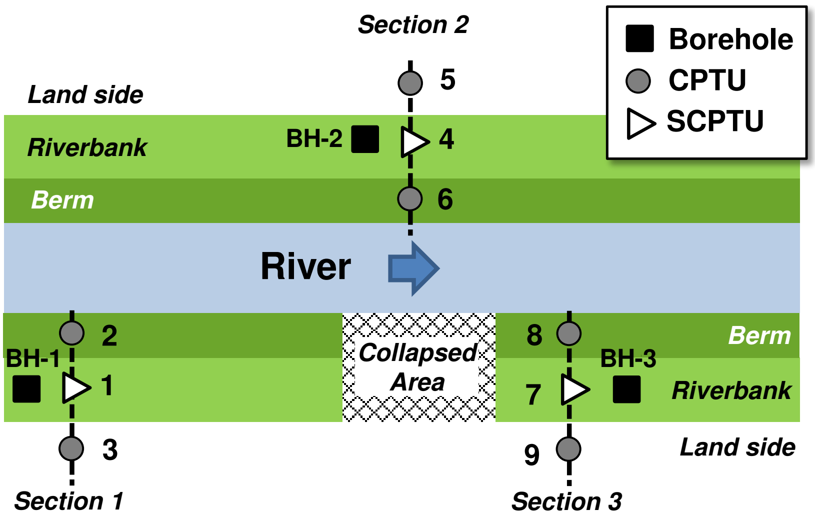


**Figure 2 -** Sketch of the investigated area with location of piezocone tests and boreholes.

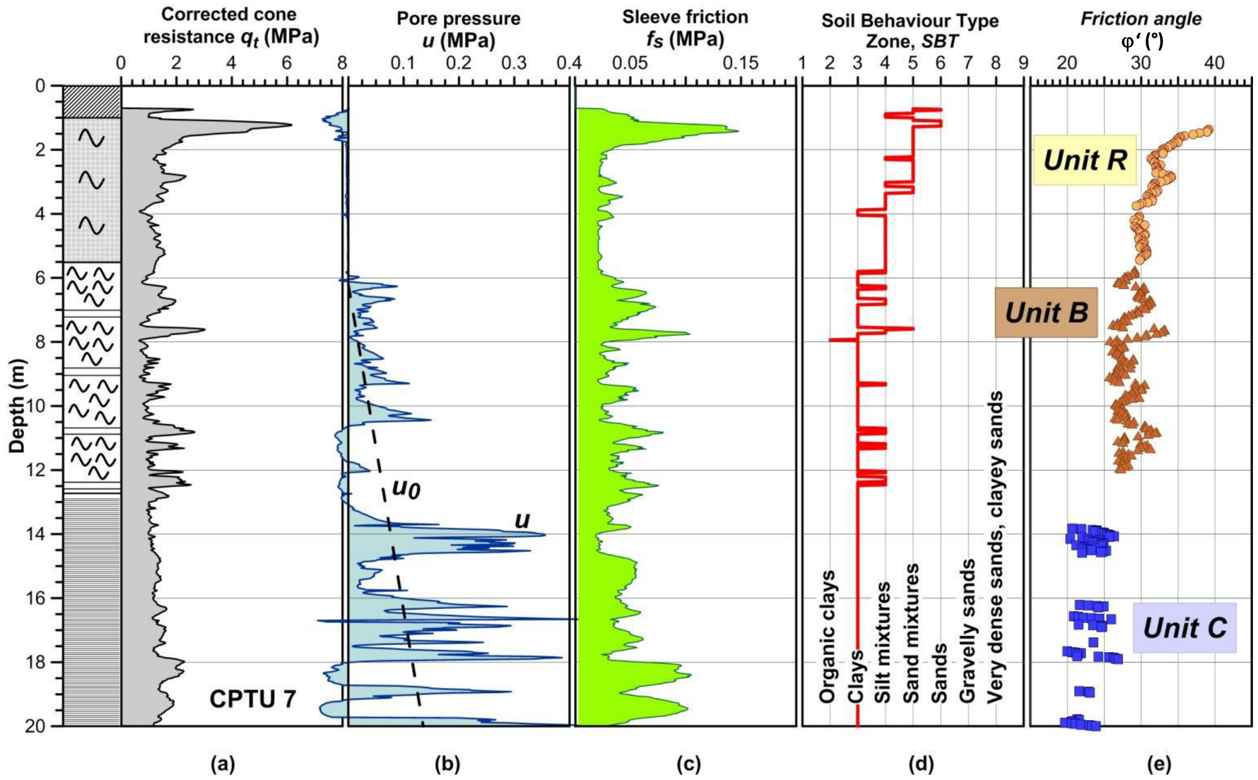


**Figure 3** - SCPTU 7 log profiles and CPTU-based soil classification.

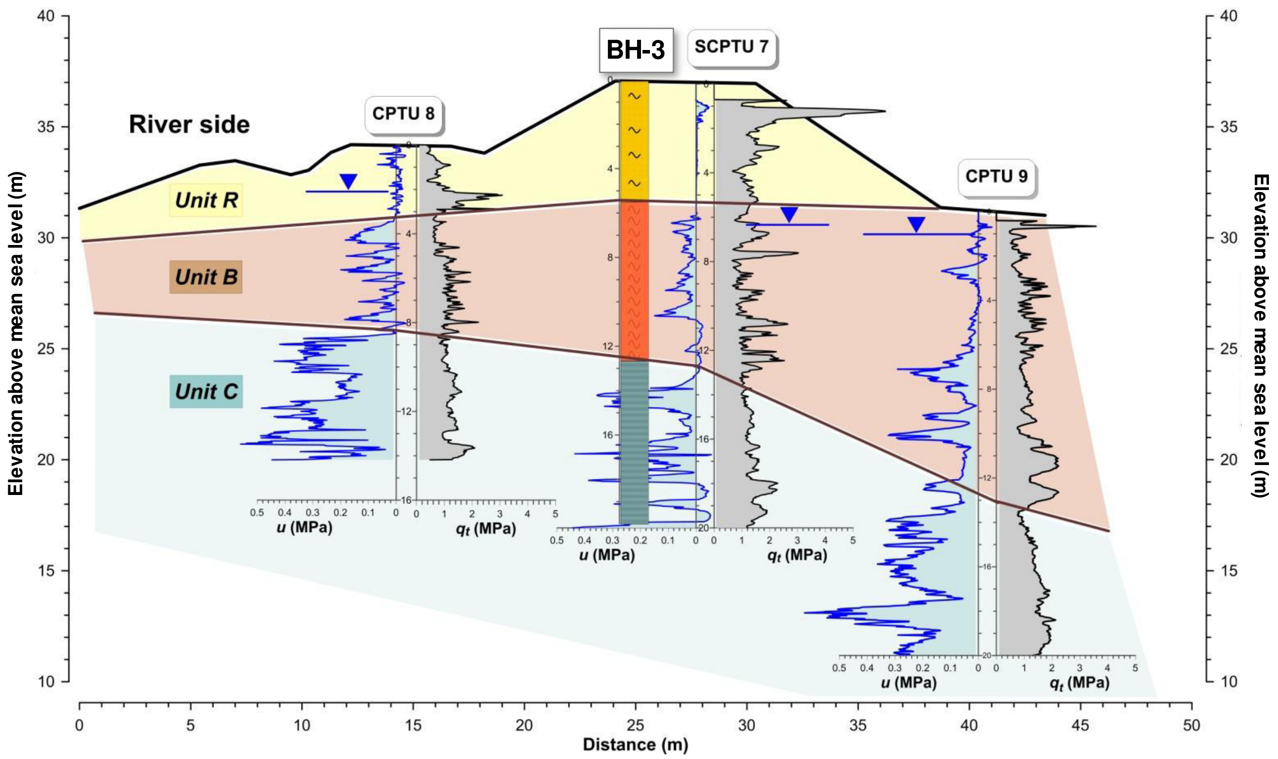


**Figure 4** - Stratigraphic model along cross-section No. 3.

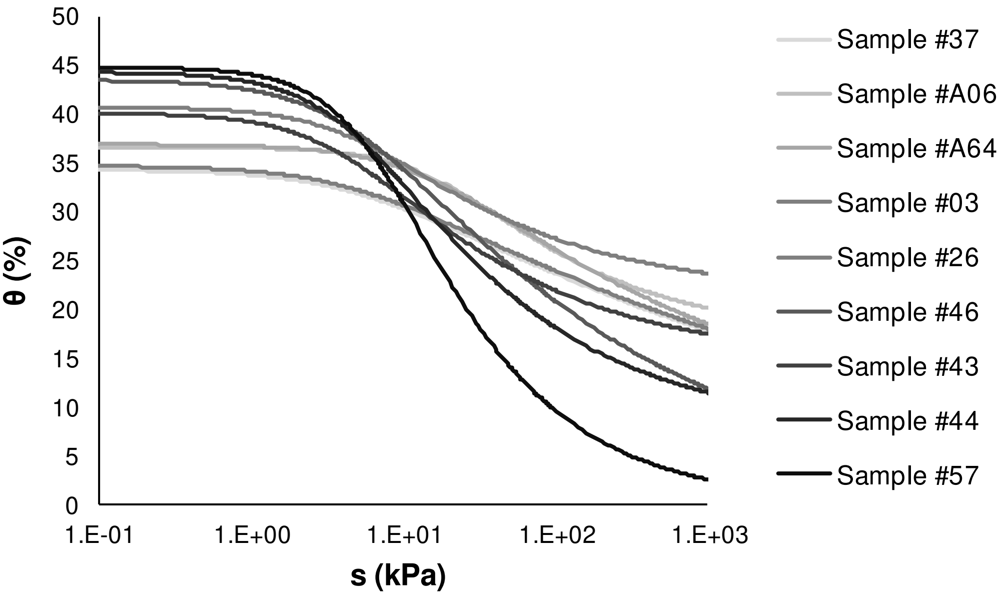


**Figure 5** – Soil water retention curves determined from laboratory experiments.

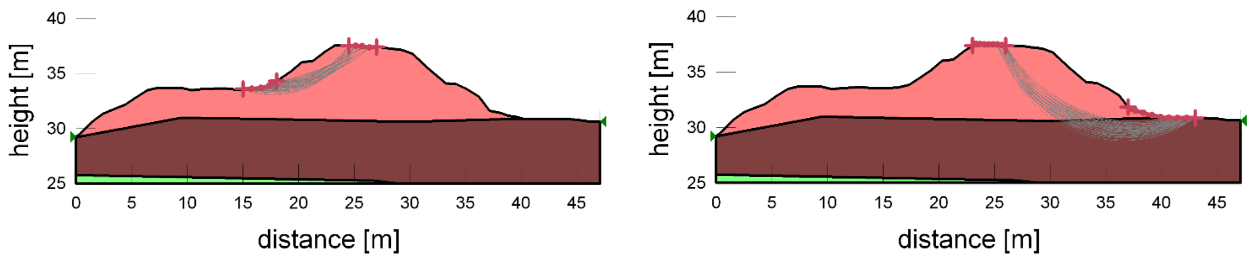


**Figure 6** – Typical slip surfaces investigated in stability analyses for inner (left) and outer (right) slopes.

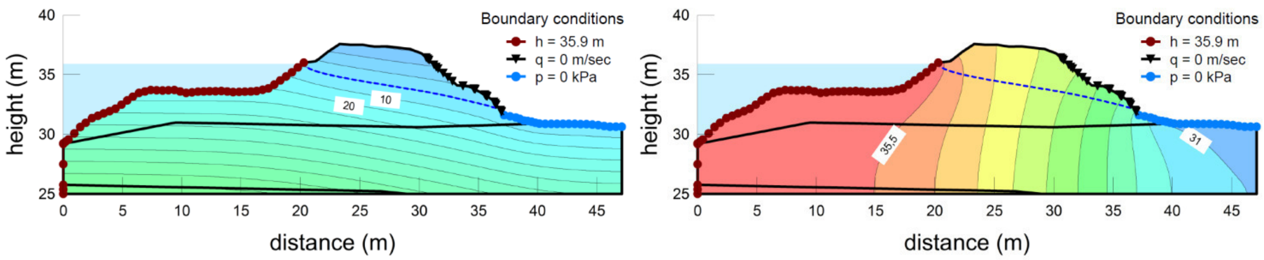


**Figure 7** – Results of the steady state seepage analysis: (left) pore water pressure distribution (isoline increment = 10 kPa) and (right) total head distribution (isoline interval = 0.5 m).

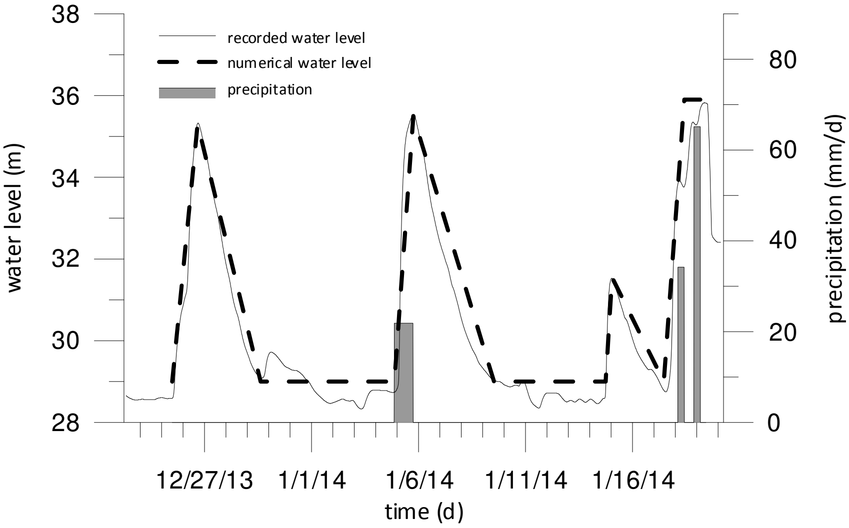


**Figure 8** – Flood hydrograph, rainfall hyetograph and numerical total hydraulic head boundary condition recorded and modelled from 25 December 2013 to 19 January 2014.

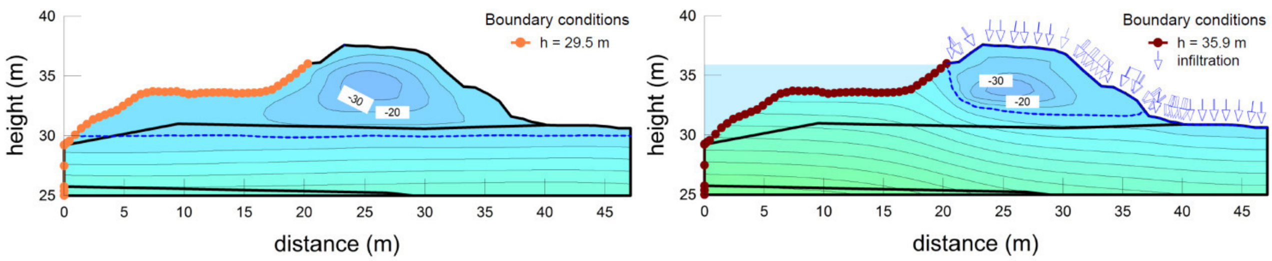


**Figure 9** – Pore water pressure distribution in the initial (left) and final (right) stage of transient seepage analysis (the increment between two adjacent isolines is 10 kPa).

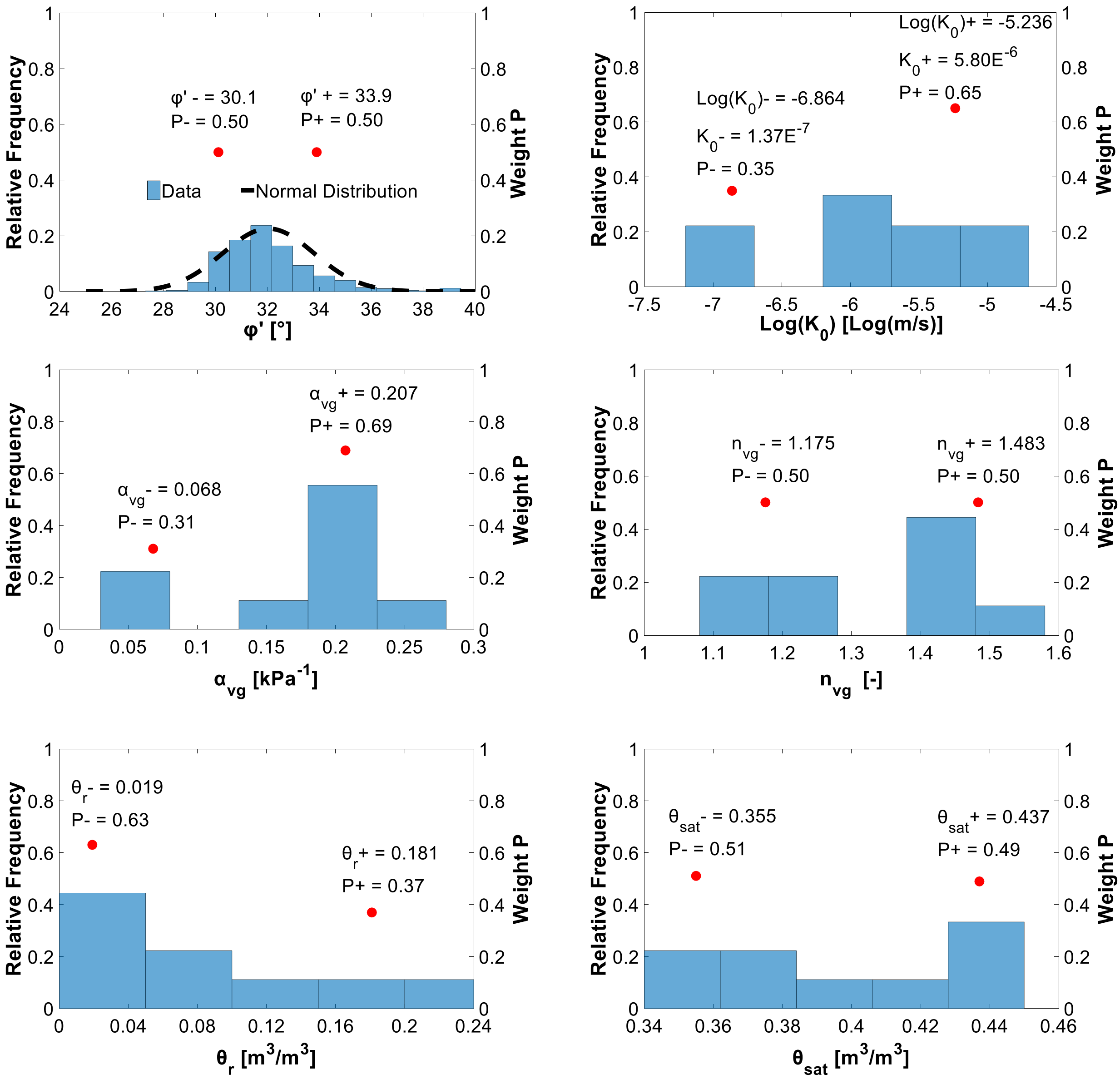


**Figure 10** – Histogram of soil parameters with point estimate locations and relative weights.

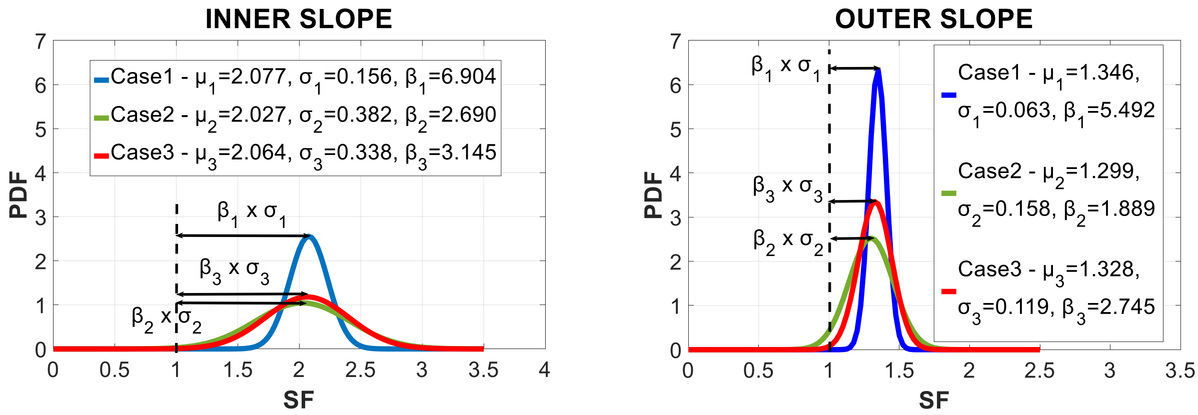


**Figure 11** – Probability density function (PDF) of the safety factor (SF) for both inner slope (left) and outer slope (right), for Case 1, Case 2 and Case 3, including the graphical estimate of the reliability index *β*.

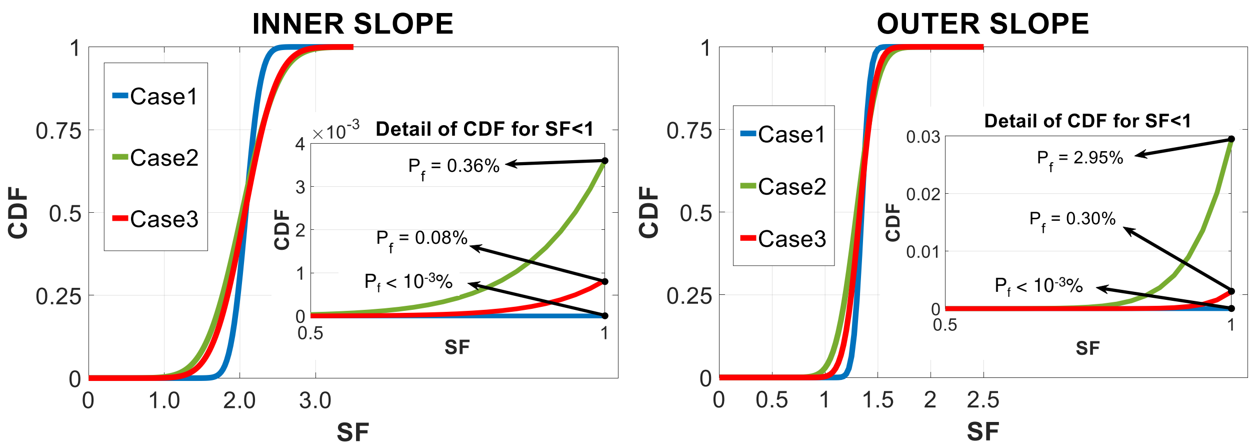


**Figure 12** – Cumulative density function (CDF) of the safety factor (SF) for both inner slope (left) and outer slope (right), for Case 1, Case 2 and Case 3, including the graphical estimate of the probability of failure $P_f$.

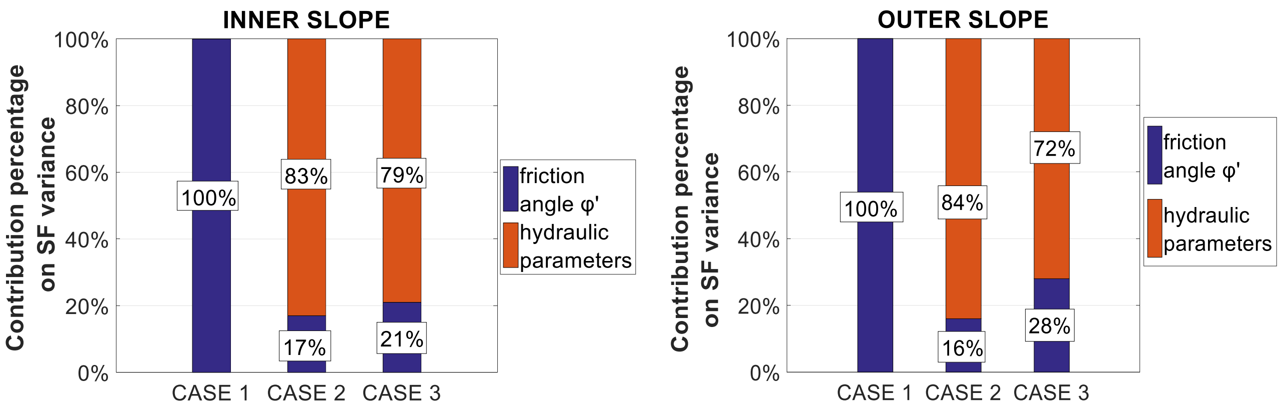


**Figure 13** – Contribution of the hydraulic parameters and shear strength φ' on the safety factor variance, for both inner slope (left) and outer slope (right).

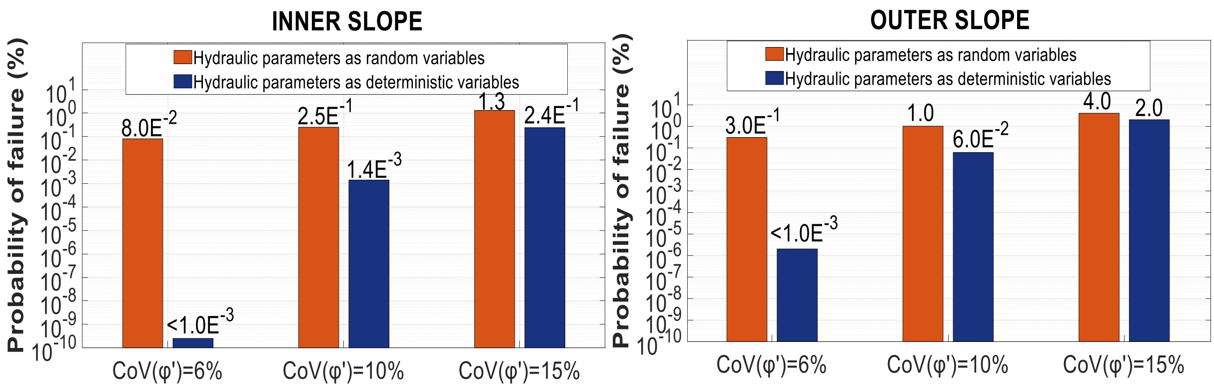


**Figure 14** – Probability of failure vs. coefficient of variation of φ', for both inner slope (left) and outer slope (right), considering the hydraulic parameters as deterministic and as random variables.